

Thermodynamic signatures of the field-induced states of graphite

D. LeBoeuf^{1,*}, C. W. Rischau², G. Seyfarth^{1,4}, R. Küchler³, M. Berben⁵,
S. Wiedmann⁵, W. Tabis^{1,6}, M. Frachet¹, K. Behnia², and B. Fauqué^{2,7,†}

¹ *Laboratoire National des Champs Magnétiques Intenses (LNCMI-EMFL),
CNRS ,UGA, UPS, INSA, Grenoble/Toulouse, France*

² *ESPCI ParisTech,
PSL Research University; CNRS; Sorbonne Universités,
UPMC Univ. Paris 6; LPEM,*

10 rue Vauquelin, F-75231 Paris Cedex 5, France

³ *Max Planck Institute for Chemical Physics of Solids,
Nöthnitzer Str. 40, 01187 Dresden, Germany*

⁴ *Université Grenoble-Alpes, Grenoble, France*

⁵ *High Field Magnet Laboratory (HFML-EMFL) and Institute for Molecules and Materials,
Radboud University, Toernooiveld 7,
6525 ED Nijmegen, The Netherlands*

⁶ *AGH University of Science and Technology,
Faculty of Physics and Applied Computer Science,
30-059 Krakow, Poland*

⁷ *JEIP, USR 3573 CNRS, Collège de France,
PSL Research University, 11, place Marcelin Berthelot,
75231 Paris Cedex 05, France.*

(Dated: October 21, 2021)

When a magnetic field confines the carriers of a Fermi sea to their lowest Landau level, electron-electron interactions are expected to play a significant role in determining the electronic ground state. Graphite is known to host a sequence of magnetic field-induced states driven by such interactions. Three decades after their discovery, thermodynamic signatures of these instabilities are still elusive. Here, we report the first detection of these transitions with sound velocity. We find that the phase transition occurs in the vicinity of a magnetic field at which at least one of the Landau level crosses the Fermi energy. The evolution of elastic constant anomalies with temperature and magnetic field allows to draw a detailed phase diagram which shows that the ground state evolves in a sequence thermodynamic phase transitions. Our analysis indicates that electron-electron interaction is not the sole driving force of these transitions and that lattice degrees of freedom play an important role.

A magnetic field can induce unusual electronic ground states, such as the quantum Hall effect for a two-dimensional (2D) electron gas. In the limit where only the $n=0$ Landau level is populated (the so-called quantum limit), electron interactions are responsible for the appearance of a variety of many-body ground states such as the fractional quantum Hall effect [1]. In contrast to the two-dimensional case, the electrons in the quantum limit of a three-dimensional (3D) gas have the ability to move along the direction of the magnetic field. As a consequence, the energy spectrum of the system becomes analogous to a one-dimensional (1D) spectrum in the vicinity of the quantum limit. A variety of electronic instabilities driven by the electron-electron interactions, which may arise in this context, have been proposed [2–4].

In the early 80's, one phase transition induced by a magnetic field was discovered in graphite [5] (see [6, 7] for reviews). The field induced state describes a dome

in the temperature - magnetic field phase diagram. The onset field of this phase varies with temperature, and is 34 T at 4.2K. The dome closes at a temperature independent field of 53 T or so, called re-entrance field. Despite numerous studies, the nature of the order parameter and the role of electron-electron interactions in this transition is still debated. Due to the variety of degrees of freedom competing for the ground state (orbital, spin and valley), several instabilities have been proposed over the years: charge [8, 9] and spin [10], density wave (respectively labelled CDW and SDW) and more recently excitonic phases [11, 12]. In this article we name this phase with the generic expression density wave (DW) since the precise nature of this phase has not been yet settled.

With the notable exception of a study of Nernst coefficient [13], the experimental exploration of these instabilities has been limited to measurements of charge conductivity. A study of the field dependence of magnetization failed to report a convincing signature for these instabilities [11, 14]. Here we present the study of elastic properties of Highly Oriented Pyrolytic Graphite (HOPG) with ultrasound measurements. Combined with electrical transport measurements, they lead to a rich phase diagram characterized by a sequence of thermodynamic

*david.leboeuf@lncmi.cnrs.fr

†benoit.fauque@espci.fr

phase transitions. Four transitions are observed: the onset and disappearance of the DW state, and two additional transitions occurring within the ordered state. The DW state appears through a second order phase transition. At higher fields, a first-order transition within the DW dome is observed, which is reminiscent of lock-in transition of the density modulation, a common feature in CDW systems[17]. Our analysis of the DW onset transition reveals that the electron-phonon interaction should be taken into account in theoretical models in addition to electron-electron interactions. The interaction of electrons with the lattice may favor a DW phase with an in-plane component modulation reminiscent of the CDW state [15, 16] and excitonic state [18] proposed in the case of graphene .

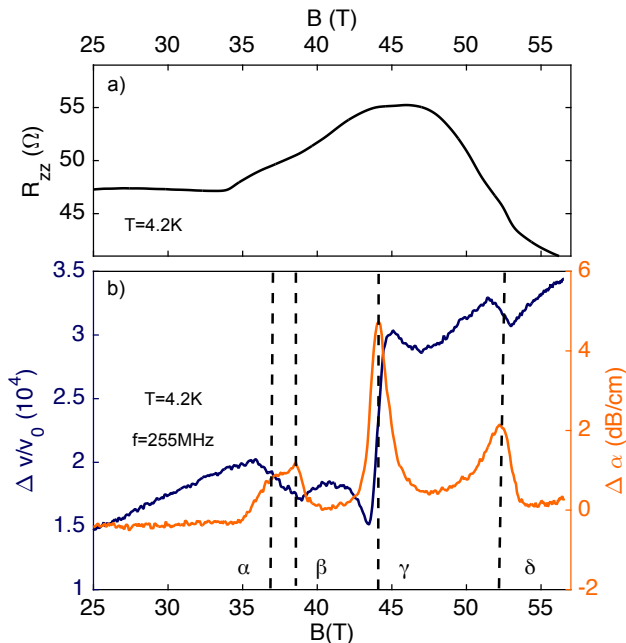


FIG. 1: Upper panel: c-axis magnetoresistance (R_{zz}) as a function of magnetic field B , oriented parallel to the c-axis in HOPG graphite, measure at 4.2 K. Lower panel : elastic properties of HOPG for $B \parallel c$ at 4.2 K: the sound velocity ($\frac{\Delta v}{v_0}$ in dark blue) and attenuation ($\Delta\alpha(\omega)$ in orange) change for the longitudinal acoustic mode c_{33} propagating along the c-axis, at a frequency $f=255$ MHz.

Early ultrasound experiments on HOPG performed up to 2T documented quantum oscillations in sound velocity change, $\Delta v/v$ and in sound attenuation change $\Delta\alpha(\omega)$ [19, 20]. In the low frequency limit, or static limit, the sound velocity v_{33} measured here, corresponding to a longitudinal mode propagating along the c-axis of the hexagonal lattice, is given by $v_{33} = \sqrt{\frac{c_{33}}{\rho}}$, where ρ the mass density and c_{33} the corresponding elastic constant, using Voigt notation. In the static limit, the sound velocity is hence a second derivative of the free-energy, as specific heat or thermal expansion. As such the sound velocity is

a thermodynamic probe [21]. At finite frequency dispersion effects do renormalize the sound velocity, because of the coupling of sound waves with internal degrees of freedom. Hence at a second order phase transition we expect two contributions to the sound velocity. First, the thermodynamic discontinuity in the elastic constant, linked to the discontinuities in the isobaric specific heat and thermal expansion through the Ehrenfest relations. The other contribution comes from the coupling to fluctuations and relaxation of the order parameter with characteristic lifetime τ [22]. The static or thermodynamic limit is achieved when $\omega\tau \ll 1$. The distinction between those two contributions will prove useful below.

Fig.1 compares the magnetoresistance with the field dependence of the ultrasound data $\frac{\Delta v}{v_0}$ and $\Delta\alpha(\omega)$ at $T = 4.2$ K and at a frequency $f = 255$ MHz (see SM section A for detailed information on the ultrasound and transport measurements). At $T=4.2$ K, a sharp increase of R_{zz} is observed close to 34T, followed by a subsequent decrease, just before the re-entrance field $B = 53$ T, where the DW disappears. As the temperature increases, the onset shifts towards higher fields. A sequence of anomalies in $\frac{\Delta v}{v_0}$ (jumps and changes of slope) concomitant with peaks in $\Delta\alpha(\omega)$ are clearly visible. Each peak in the attenuation is associated with an anomaly in the sound velocity which signals a phase transition. Different kind of anomalies can be observed in the sound velocity at a phase transition depending on the coupling between the order parameter and the lattice. The comparison between magnetoresistance and ultrasound demonstrates the sensitivity of ultrasound measurements: broad and smooth structures in the resistivity appear as sharp and very well-defined anomalies in ultrasound measurements.

Using magneto-transport data, Yaguchi et al. [23], identified and labeled four phase transitions as α , β , γ and δ . Here, we follow their convention to label the ultrasound anomalies as shown in Fig. 1. In combination with resistivity measurements (shown in SM Section B) the ultrasound measurements reported here lead to a detailed phase diagram of the high field states of graphite presented in a semi-log plot in Fig.2. Before discussing in details the various phases present in the phase diagram, let us make a number of comments on its general shape. We distinguish two main domes: dome A and dome B. Our ultrasound study is restricted to dome A. When increasing the magnetic field the first phase boundary that is crossed is associated with the α transition of dome A. Its boundary forms an almost straight line in the $(B^{-1}, \log(T))$ plane, as seen in red in Fig. 2. This means that the critical temperature and magnetic field, respectively T_0 and B_0 , are linked together through a simple formula: $T_0 = T^* \exp(-B^*/B_0)$, where T^* is a temperature scale associated with the Fermi energy, and B^* a field associated with the Landau level dispersion along the field direction [8]. This is similar to a BCS expression in which the density of states is proportional to the magnetic field, presumably due to the field-linear degeneracy of the Landau levels. Dome A peaks at 50 T,

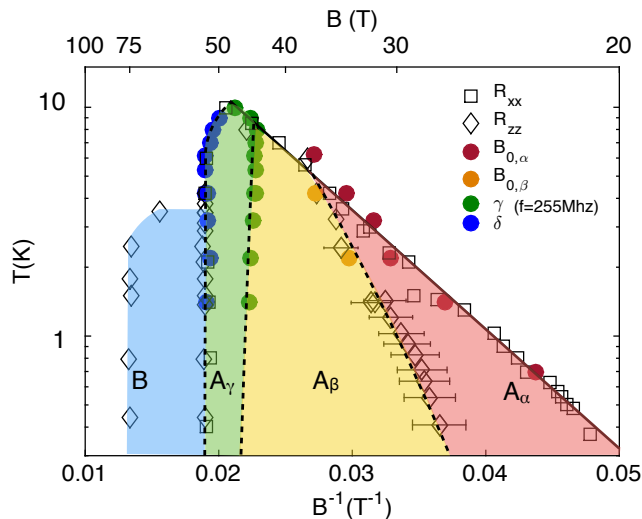


FIG. 2: $(B^{-1}, \log(T))$ phase diagram of graphite. Two main domes labeled dome A and dome B are found as a function of magnetic field. Dome A consists in a sequence of electronic phases labeled $A_{\alpha, \beta, \gamma, \delta}$ separated by thermodynamic phase transition lines respectively labeled α, β, γ and δ , as shown in Fig. 1. In this work we determined those transition lines with ultrasound measurements (full circles) and transport measurements (R_{xx} and R_{zz} in black open squares and diamonds respectively). The field scales $B_{0, \alpha}$ and $B_{0, \beta}$ correspond to the ultrasound anomaly at the α and β transitions extrapolated at zero frequency using the Landau-Khalatnikov formula (see text). Values reported for γ transition are taken at 255 MHz, and the δ transition shows a negligible frequency dependence. The black line associated with the α transition corresponds to the behavior expected from a BCS-like description of the DW transition [8]. Dotted lines are guide to the eyes for the β , γ and δ -transition lines. Boundaries of dome B has been determined previously using R_{zz} [24].

with a maximum $T_c = 10$ K and then ends at a vertical phase boundary at 53 T, shown by blue data points in Fig. 2. The subsidiary phases of dome A are labeled A_{α} , A_{β} and A_{γ} . The destruction of phase A leads to another field-induced state, called B. Dome B collapses abruptly at 75T and has a maximum $T_c = 3.5$ K[24].

Below we describe the new information that the ultrasound attenuation and velocity yield regarding each of the phase boundaries associated with dome A. The discussion is centered around comparison of in-plane and out-of-plane magnetoresistance shown in Fig. 3, and temperature and frequency dependence of ultrasound properties as a function of magnetic field, that are shown in Fig.4 and 5.

α and β transitions : The onset of the transitions in the in-plane resistance, R_{xx} , and the c-axis resistance, R_{zz} is illustrated in Fig. 3 at low temperatures. When the field is increased, R_{xx} first sharply rises, then plateaus and finally increases again. The two successive increases have been attributed to two successive transitions labeled, α and β -transition [23]. In contrast R_{zz} does not

show a plateau, and only increases above a magnetic field close to the β -transition. As previously noticed [25], the α -transition barely affects R_{zz} .

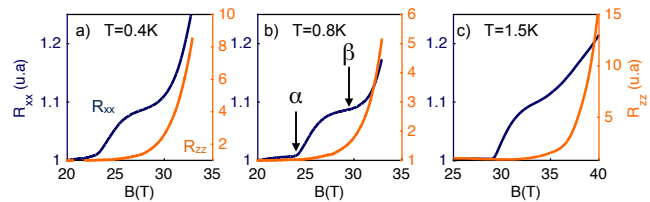


FIG. 3: Comparison of the in-plane (R_{xx} in blue) and c-axis (R_{zz} in orange) magnetoresistance in Kish graphite at a) 0.4 K, b) 0.8 K and c) 1.5 K. The magnetic field is oriented along the c-axis. For clarity the curves are normalized to their values at $B=20$ T for a), b) and $B=25$ T for c).

The first two peaks observed in the sound attenuation can naturally be attributed to the α and β transitions. However the transition fields in ultrasound measurements differ slightly from transport measurements. As shown in Fig.5 a) and b), the magnetic field at which the α and β attenuation peaks occur at a certain temperature actually depends on the frequency of the sound wave. The magnetic field positions of the attenuation peak at the α transition is plotted as a function of frequency, for different temperatures ranging from 0.7 to 6.2 K, and shown in Fig. 5 c). Each isotherm is well described by a simple formula:

$$f = f_0 \left(\frac{B}{B_0} - 1 \right) \quad (1)$$

Eq.1 is characteristic of an order-parameter relaxation process described by the so-called Landau-Khalatnikov (LK) theory [26, 28] first applied to sound propagation just below the λ -transition in He^4 [27]. The LK theory has been successfully applied since then to various kinds of transitions ranging from liquid/gas[28], nematic/smectic [29], ferroelectric [30] and ferromagnetic transitions [31] (see [28] for a review). The observation of such a relaxation mechanism is a first evidence that a static, long-range, 3-dimensional order parameter appears at the α -transition in graphite. Below the critical temperature T_c , when the sound wave frequency f matches the order parameter relaxation rate $1/\tau_0$ so that $2\pi f\tau_0 = 1$, the energy absorption is the highest and an excess attenuation is expected just below T_c . In the case of the λ -transition, as the temperature gets closer to T_λ , τ is diverging as $\frac{\tau_0}{1-T/T_\lambda}$ and the maximum in ultrasound absorption shifts further away from T_λ as the frequency increases. Translating this theory to a field-induced phase, the temperature is replaced by the magnetic field and the transition occurs above the critical field B_0 leading to Eq.1. We report on Fig. 2 the temperature dependence of $B_0(T)$ for the α and β transitions. The comparison between the ultrasound and transport

measurements shows that $B_{0,\alpha}$ matches with the first anomaly in R_{xx} while $B_{0,\beta}$ matches the second anomalies in R_{xx} (concomitant with the large increase in R_{zz}).

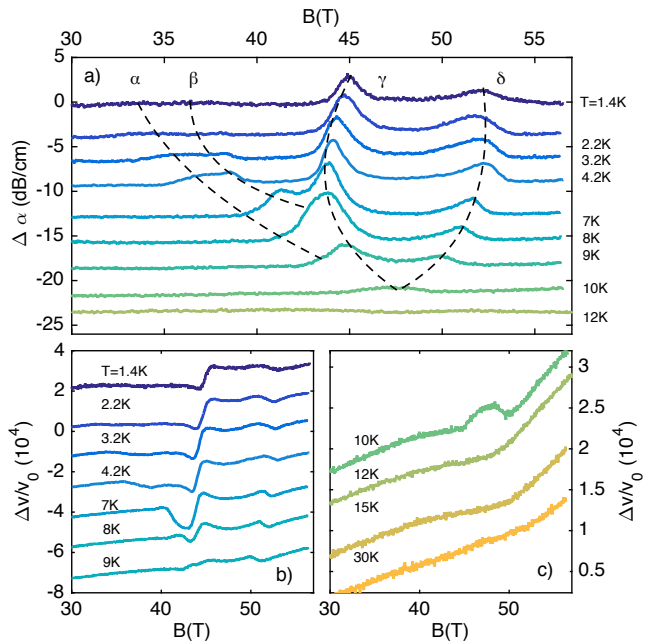


FIG. 4: Temperature dependence of the elastic properties of graphite : a) Attenuation as a function of B for $f=255$ MHz and temperature ranging from 1.4K to 12K. The dashed lines are eye-guiding to illustrate the temperature dependence of the α , β , γ and δ -transitions. The temperature dependence of $\frac{\Delta v}{v_0}$ is shown in b) and c) from 1.4K to 9K and from 10K to 20K, respectively. Full data set is reported in SM Fig. S1.

We note that the characteristic order parameter relaxation rate $1/\tau_0 \approx 8 \times 10^8$ Hz found here at $B_\alpha = 36.1$ T (see SM section C) is small compared to a magnetic transition such as in Ni [31] where $1/\tau_0 \approx 10^{14}$ Hz but it is large in comparison with the CDW phase of NbSe₂ where $1/\tau_0 \approx$ kHz due to the coupling between the CDW and discommensuration domains [32]. As discussed in section C of the SM, this intermediate relaxation time can be either the result of the coupling of the DW with the lattice or with collective excitations of the DW condensate.

In figure 5 b, we see that the location of the attenuation maximum associated with the β transitions has a similar frequency dependence to that of the α transition. This indicates that the β transition, which does not show hysteresis within our resolution, is a second order transition. However, figure 5 a shows that the attenuation peak for the β transition increases more rapidly than that of the α transition as a function of frequency. Different behaviours at the two transitions are also found in the sound velocity. In Fig. 1, one observes that the α attenuation peak coincides with the mid-point of a negative step-like anomaly in the sound velocity. Such an anomaly in the elastic constant is another evidence for the occurrence of a phase transition. It occurs at a sec-

ond order phase transition, when the square of the order parameter couples linearly with the strain in a Landau theory [21]. On the other hand, the β transition shows up as a change of slope in the sound velocity. This indicates that the β transition involves a different order parameter - strain coupling.

The amplitude of the jump is best measured at low frequency in the static or thermodynamic limit where $2\pi f\tau_0 \ll 1$, and where dispersion effects are negligible. We find for the α -transition $\frac{\Delta v}{v_0} = \frac{\Delta c_{33}}{2c_{33}(B=0)} = -3 \times 10^{-5} \pm 2 \times 10^{-5}$ at 4.2K and for $f = 36$ MHz (see Fig. S1). In the discussion section we will examine the amplitude of this jump. We note that an anomaly in the magnetostriction along the c -axis should in principle also exist, but, as explained in the SM section D, we were not able to resolve it in our measurement of L_{33} , the dimension of the sample along the c -axis. For $T < 4.2$ K the anomalies in the sound velocity at the α and β transition loses amplitude as temperature is decreased as shown in Fig. 4b. This is due to the fact that as the critical temperature for the transitions decreases, the thermodynamic contribution decreases through reduction of the specific heat.

γ -transition:

The γ -transition differs from other transitions regarding its temperature and frequency dependence. In contrast with the α and β -transition, the γ -transition is almost temperature independent much like the δ -transition (see Fig. 4 a) and b)). But its frequency dependence (reported on Fig. 5) b)) differs from the α , β and δ -transitions. As the field increases we observe a hardening at the γ -transition i.e, an opposite behavior compared to the α and δ -transitions. The γ -transition differs as well in its signature in transport properties. As seen in Fig.1, the γ -transition has, by far, the largest effect on the elastic properties of graphite, while its signature in R_{zz} is small compared to the other transitions. Nonetheless, former in-plane magnetoresistance studies [9, 23] identified temperature independent anomalies close to $B \approx 45$ T (where R_{xx} changes slope) and have been associated with a theoretically predicted lock-in transition of a CDW order along the c -axis [9]. On the other hand, close to the γ transition R_{zz} has a maximum which has been recently linked with the formation of an excitonic phase[12]. Our observation of a large change in the elastic properties inside dome A supports the lock-in scenario of Ref. [9] implying a field dependence of the wave vector modulation of the DW. As in the case of 2H-TaSe₂, the lock-in transition is almost invisible through transport measurements, but gives the most dramatic effect in elastics properties [32]. Furthermore, by comparing $\frac{\Delta v(B)}{v_0}$ measured in field-up and field-down sweeps (shown in Fig.5 d)), we find that the γ -transition is characterized by an hysteresis loop, which suggests that it is of a first order nature, contrary to the α transition. We note however that we did not reach the static limit for this transition. The hysteresis loop could alternatively originate from other effect such as the pinning of the CDW.

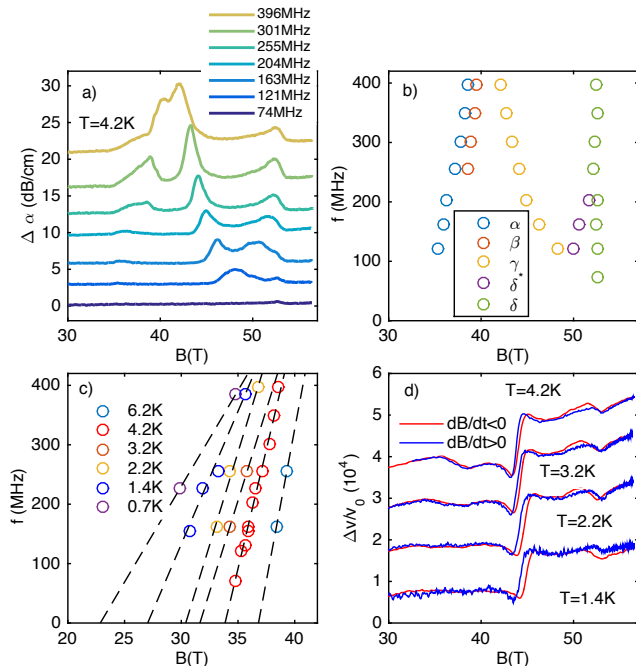


FIG. 5: a) Field dependence of the sound attenuation at $T=4.2$ K for sound frequencies ranging from 74 MHz to 396 MHz b) Frequency - magnetic field phase diagram of the peak position shown in a). c) Position of the first attenuation maximum as function of the frequency for temperatures ranging from 6.2 K down to 0.7 K. The dashed lines are linear fits to Eq. 1. d) Sound velocity hysteresis at γ and δ transitions. The red and blue curves correspond to the field-down and field-up sweeps at $f = 255$ MHz, respectively. No hysteresis is observed for the α and β transition.

δ -transition: In contrast to the three other transitions discussed so far, the δ -transition is almost both temperature and frequency independent. A weak hysteresis loop is found in the sound velocity at the δ transition, as shown in Fig 5 d, indicating it has a first order character. The δ -transition corresponds to the re-entrance field, as determined by transport measurements. This re-entrance has been theoretically attributed to Landau levels (LL) depopulation [34]. We studied the elastic properties above the maximum T_c of dome A and the data are shown in Fig. 4 c. At 10 K, the field-induced state arises on top of a local softening or minimum in the sound velocity, which is observed even above at 12 and 15 K, i.e. above the maximum T_c . This softening is similar to a LL crossing in the sound velocity, as observed at lower fields (see section A of the SM). The asymmetric shape of the δ attenuation peak in the field-induced state, characteristic of a LL crossing, further supports this interpretation. The LL depopulation observed here removes the density of states necessary for the DW state to condense which consequently collapses abruptly at the LL crossing. The δ transition thus corresponds to the disappearance of the

DW state at a first order phase transition, caused by a LL crossing. We note that below 200 MHz, an additional structure, labeled δ^* in Fig. 5 b, appears and merges at 100 MHz with the γ -transition and could be associated with the disappearance of either the α or β phase.

Discussion:

In the case of graphite it is generally assumed that the DW forms as a result of a nesting process along the magnetic field direction driven by electron-electron interactions [8]. In that picture the DW modulation runs along the magnetic field axis with a modulation vector that evolves as a function of magnetic field [9]. Here we show that electron-electron interactions are indeed at work. According to theory, in the absence of electron-electron interactions, the depopulation of the LL $(0,+)$ and $(-1,-)$ is expected to occur at a magnetic field significantly larger than 55 T [35]. Once the exchange and correlation effects are included, the bare LL spectrum is renormalized and the depopulation of the LL $(0,+)$ and $(-1,-)$ occurs almost simultaneously at around 52-54 T [9, 35], close to the softening observed in $\Delta v/v_0$ at 12 and 15 K. According to our measurements, the critical temperature is the highest in the vicinity of a LL depopulation, a limit where the interactions have the strongest influence [36]. The amplitude of the sound velocity jump at the α -transition is an order of magnitude smaller than the one found at the SDW transition of PF_6 [33] and two orders of magnitude smaller than the one found at the incommensurate CDW state of 2H-TaSe_2 [32] but it is surprisingly high for a system with a carrier concentration four orders of magnitude smaller than these metals. As discussed in section E of the SM, the large amplitude of the sound velocity anomaly measured at the α -transition suggests that the lattice degrees of freedom are also involved in the DW instability. This unexpected contribution rises several questions and call for further works. What is the amplitude of the specific heat jump at the DW transitions and the respective contribution of electrons and phonons? Our measurement of c_{33} indicates that the DW instabilities are coupled to c -axis strain. Could the electron-phonon interaction also induce an in-plane lattice deformation along with the c -axis nesting process as suggested by early theoretical works [37, 38]? Could an in plane lattice deformation explain why the α -transition appears in R_{xx} but only weakly in R_{zz} as shown in Fig 3?

In conclusion, we show the first thermodynamic signatures of the electronic instabilities induced by a magnetic field in graphite. The dominant lattice response occurs within the dome with an hysteresis behavior, which is reminiscent of a lock-in transition of the density modulation, a common feature in CDW systems. While the wave vector direction of the DW state remains to be determined, our thermodynamic data and analysis indicate that both the electron-electron and the electron-lattice interactions should be accounted for in theoretical models. Finally, we note that CDW [15, 16] or excitonic [18] states induced by a magnetic field have been proposed

in graphene layers. Our results offer an appealing perspective to the fate of these ground states when the third

direction is switched on.

-
- [1] D. Yoshioka, *The Quantum Hall effect*, (Springer, New York, 2001)
- [2] V. Celli and N. D. Mermin, *Phys Rev.* **40**, A 839 (1965)
- [3] A. H. MacDonald et al., *Phys. Rev. Lett* **58**, 515 (1987)
- [4] B. I Halperin, *Japanese Journal of Applied Physics* **26** (1987)
- [5] S. Tanuma et al., in *Physics in High Magnetic Fields*, ed. S. Chikazumi and N. Miura (Springer, Berlin 1981).
- [6] H. Yaguchi and J. Singleton, *J. Phys. Condens. Matter* **21**, 344207 (2009).
- [7] B.Fauqué and K. Behnia, *Basic Physics of Functionalized Graphite*, (Springer, New York, 2016)
- [8] D. Yoshioka and H. Fukuyama, *J. Phys. Soc. Jpn.* **50**, 725(1981).
- [9] F. Arnold and al., arXiv:1411.3323 preprint at <http://xxx.lanl.gov/pdf/1411.3323.pdf>
- [10] Y Takada and H Goto, *J. Phys.: Condens. Matter* **10** (1998)
- [11] K. Akiba and al., *JPSJ* **84** 054709 (2015)
- [12] Z. Zhu and al., arXiv:1508.03645 preprint at <http://lanl.arxiv.org/abs/1508.03645>
- [13] B.Fauqué et al, *Phys. Rev. Lett.* **106**, 246405 (2011)
- [14] S. Uji, J.S Brooks, Y. Iye, *Physica B* **246**, 299 (1998)
- [15] J.N. Fuchs and P. Lederer, *Phys. Rev. Lett.* **98**, 016803 (2007)
- [16] K. Nomura, S. Ryu and D-H Lee, *Phys. Rev. Lett.* **103**, 216801 (2009)
- [17] P. Monceau and G. Gruner, *Charge Density Waves in Solids, Modern Problems in Condensed Matter Sciences*, Vol. 25 (1989)
- [18] D.V Khveshchenko, *Phys. Rev. Lett.* **87**, 246802 (2001)
- [19] T. Fukami, T. Inoue and S. Mase, *JPSJ*, **48**, 448 (1980).
- [20] T. Inoue, T. Fukami, H. Kuriyaki and S. Mase, *JPSJ*, **52**, 2862 (1983).
- [21] Bruno Lüthi, *Physical acoustics in the solid state*, Springer series in solid-state (2004).
- [22] C. Buchal and F. Pobell, *Phys. Rev. B* **14**, 1103 (1976)
- [23] H. Yaguchi, Y. Iye, T. Takamasu and N. Miura, *Physica B* **184**, 332 (1993).
- [24] B.Fauqué et al, *Phys. Rev. Lett.*, **110**, 266601 (2013)
- [25] Y. Iye and G. Dresselhaus, *Phys. Rev. Lett.* **54**, 1182 (1985)
- [26] L. D. Landau and I. M. Khalatnikov *Dokl. Akad. Nauk. SSSR* **96**, 469 (1954)
- [27] M. Barmatz and I. Rudnick, *Phys. Rev.* **170**, 224 (1968)
- [28] C. W. Garland, *Physical Acoustics* **7**, 52 (1970)
- [29] S. Battacharya *et al.*, *Phys. Rev. B* **23**, 2397 (1980)
- [30] C. W. Garland and D. B. Novotny, *Phys. Rev.* **177**, 971 (1969)
- [31] B. Golding, *Phys. Rev. Lett.* **55**, 2479 (1969)
- [32] M. Barmatz, L. R. Testardi and F.J. Di Salvo, *Phys. Rev. B*, **12**, 4367 (1975).
- [33] S. Zherlitsyn et al., *Phys. Rev. B*, **59**, 13861 (1999).
- [34] H. Yaguchi and J. Singleton, *Phys. Rev. Lett.* **81**, 5193 (1998).
- [35] Y. Takada and H. Goto, *J. Phys.: Condens. Matter* **10** 11315 (1998).
- [36] J. Alicea and L. Balents, *Phys. Rev. B* **79**, 241101(R) (2009)
- [37] W. G Kleppman and R.J Elliot, *J. Phys. C* **8**, 2729 (1975).
- [38] H. Fukuyama, *Solid State Communications* **26**, 783 (1978).

Methods

The ultrasound measurement have been performed on Highly Oriented Pyrolytic Graphite (HOPG) samples grade ZYA that were purchased from Momentive Performance Materials. Longitudinal ultrasonic waves were generated using commercial LiNbO₃ 36° Y-cut transducers glued on a fresh cleaved surface. The magnetic field was aligned along the c-axis. Experiments have been conducted in both static field at the HMFL, Nijmegen up to 37.5 T, and pulsed field at the LNCMI-Toulouse up to 58 T. In both case standard pulse-echo technique was used to determine the change in the sound velocity and attenuation. In total four different samples were studied at different stage of this project. These measurements have been completed with additional magnetostriction and transport measurements on the same HOPG samples and on Kish graphite samples (see SM for the details).

Acknowledgments

This work is supported by the Agence Nationale de Recherche as a part of the QUANTUMLIMIT project, and as part of the UNESCOS project (contract ANR-14-CE05-0007), by a grant attributed by the Ile de France regional council, by the Laboratoire d'excellence LANEF in Grenoble (ANR-10-LABX-51-01) and by Université Grenoble-Alpes (SMIng - AGIR). We acknowledge support from the LNCMI and the HFML which are both members of the European Magnetic Field Laboratory. BF acknowledges support from Jeunes Equipes de l'Institut de Physique du Collge de France (JEIP). We thank P. Littlewood, P. Monceau, and J-Y Prieur for stimulating discussions.